

# High Performance Analysis of Shielding Current Density in High Temperature Superconducting Thin Film

Atsushi KAMITANI, Teruo TAKAYAMA and Hiroaki NAKAMURA<sup>1)</sup>

*Yamagata University, Yamagata 992-8510, Japan*

<sup>1)</sup>*National Institute of Fusion Science, Gifu 509-5292, Japan*

(Received 8 December 2009 / Accepted 1 March 2010)

A high-performance method has been proposed for calculating the shielding current density in a high-temperature superconducting thin film. After spatially discretized, the initial-boundary-value problem of the shielding current density is reduced to a system of first-order ordinary differential equations that has a strong nonlinearity. However, the system cannot be always solved by means of the Runge-Kutta method even when an adaptive step-size control algorithm is incorporated to the method. In order to suppress an overflow in the algorithm, the following method is proposed: the  $J$ - $E$  constitutive relation is modified so that its solution may satisfy the original constitutive relation. A numerical code for analyzing the shielding current density has been developed on the basis of the proposed method and the inductive method has been investigated by use of the code.

© 2010 The Japan Society of Plasma Science and Nuclear Fusion Research

Keywords: high-temperature superconductor, nonlinear equation, Newton method, Runge-Kutta method, backward Euler method

DOI: 10.1585/pfr.5.S2112

## 1. Introduction

Recently, high-temperature superconductors (HTSs) have been used for numerous engineering applications: fusion magnet, energy storage system, power cable and magnetic shielding apparatus. Since the evaluation of the shielding current density is indispensable for the design of engineering applications, several numerical methods have been so far proposed to calculate the shielding current density.

After discretized with respect to space, the governing equation of the shielding current density is reduced to a system of ordinary differential equations (ODEs). If implicit schemes such as the backward Euler method have been applied to the system, the nonlinear equations have to be solved at each time step [1–3]. However, the nonlinear equations are extremely time-consuming because of a linear term with a dense, symmetric and indefinite matrix. In this sense, the system of ODEs should be solved with the method other than implicit schemes.

The purpose of the present study is to develop a high-performance method for analyzing the time evolution of the shielding current density in a HTS thin film and to numerically investigate the inductive method [4, 5] by means of the high-performance method.

## 2. Governing Equations

A HTS thin film is exposed to the magnetic field  $\mathbf{B}/\mu_0$  where  $\mu_0$  is a magnetic permeability of vacuum. As a source of the magnetic field, an  $N_c$ -turn coil is placed just

above the film and an ac current  $I(t) = I_0 \sin 2\pi ft$  is applied in the coil. The coil is so arranged that its symmetry axis may be parallel to the thickness direction of the film. Throughout the present study, we assume that the film has a square cross section  $\Omega$  over the thickness and that the coil has a rectangular cross section. In the following,  $R_1$  and  $R_2$  denote the inner and the outer radii of the coil, respectively, and  $Z_2 - Z_1$  is the height of the coil. In addition,  $a$  and  $b$  denote the side length of  $\Omega$  and the film thickness, respectively, and  $Z_1$  is the distance between the coil bottom and the film surface. The schematic view for the configuration of the coil and the film is given in [4]. Hereafter, let us use the Cartesian coordinate system  $(\mathbf{O} : \mathbf{e}_x, \mathbf{e}_y, \mathbf{e}_z)$  in which the thickness direction is taken as  $z$ -axis and the center of the upper film surface is chosen as the origin. Furthermore, the boundary of  $\Omega$  is denoted by  $\partial\Omega$  and the symmetry axis of the coil is represented by  $(x, y) = (x_c, y_c)$ . Also, both  $\mathbf{x}$  and  $\mathbf{x}'$  denote the position vectors of two points on the  $xy$  plane.

Under the thin-plate approximation, there exists a scalar function  $S(\mathbf{x}, t)$  such that  $\mathbf{j} = \nabla \times [(2S/b)\mathbf{e}_z]$  and its time evolution is governed by the following integral-differential equation [1–3]:

$$\mu_0 \frac{\partial}{\partial t} \left( \hat{Q} + \frac{2}{b} \hat{I} \right) S = - \frac{\partial}{\partial t} \langle \mathbf{B} \cdot \mathbf{e}_z \rangle - (\nabla \times \mathbf{E}) \cdot \mathbf{e}_z. \quad (1)$$

Here,  $\langle \rangle$  represents an average operator through the thickness. In addition,  $\hat{I}$  denotes an identity operator and  $\hat{Q}$  is the operator defined by

$$\hat{Q}S \equiv \iint_{\Omega} Q(|\mathbf{x} - \mathbf{x}'|) S(\mathbf{x}', t) d^2\mathbf{x}',$$

author's e-mail: kamitani@yz.yamagata-u.ac.jp

where  $Q(r) = -[r^{-1} - (r^2 + b^2)^{-1/2}]/(\pi b^2)$ .

As is well known, the electric field  $\mathbf{E}$  and the shielding current density  $\mathbf{j}$  in a HTS thin film are closely related through the  $J$ - $E$  constitutive relation. As the relation, we assume the power law [3]:

$$\mathbf{E} = E(|\mathbf{j}|)(\mathbf{j}/|\mathbf{j}|), \quad E(j) = E_C(j/j_C)^N, \quad (2)$$

where  $j_C$  and  $E_C$  are a critical current density and a critical electric field, respectively, and  $N$  is a constant.

The initial and the boundary conditions to (1) are assumed as follows:  $S = 0$  at  $t = 0$  and  $S = 0$  on  $\partial\Omega$ . By solving the initial-boundary-value problem of (1), we can investigate the time evolution of the shielding current density in a HTS film. Note that, if  $S(\mathbf{x}, t)$  is the solution of (1) and (2), it also satisfies other  $J$ - $E$  constitutive relations. Since the magnitude  $|\mathbf{j}|$  of the shielding current density is bounded,  $S(\mathbf{x}, t)$  obviously satisfies the inequality:

$$|\mathbf{j}|/j_C \leq z_L. \quad (3)$$

Here,  $z_L$  is a positive constant. By using an arbitrary function  $E^*(j)$  such that  $E^*(j) = E(j)$  for  $j/j_C \leq z_L$ , other constitutive relations can be written as

$$\mathbf{E} = E^*(|\mathbf{j}|)(\mathbf{j}/|\mathbf{j}|). \quad (4)$$

In other words,  $z_L j_C$  is an upper bound of  $j$  below which  $E^*(j) = E(j)$  is fulfilled. Thus, we get the following proposition: if the solution of (1) and (4) fulfills (3), it also satisfies (1) and (2). By using the proposition, a high-performance method can be developed for solving the initial-boundary-value problem of (1).

Throughout the present study, the physical and the geometrical parameters are fixed as follows:  $x_c = 0$  mm,  $R_1 = 1$  mm,  $R_2 = 2.5$  mm,  $Z_1 = 0.2$  mm,  $Z_2 = 1.2$  mm,  $N_c = 400$ ,  $f = 1$  kHz,  $E_C = 1$  mV/m,  $j_C = 1$  MA/cm<sup>2</sup>,  $a = 20$  mm and  $b = 600$  nm.

### 3. Numerical Methods

After spatially discretized by means of the finite element method, the initial-boundary-value problem of (1) is reduced to the initial-value problem of the following ODEs:

$$\frac{ds}{dt} = f(t, s), \quad (5)$$

where  $f(t, s)$  is a vector-valued function defined by

$$f(t, s) \equiv -W^{-1} \left( \frac{db}{dt} + e(s) \right).$$

In addition,  $s$ ,  $b$  and  $e(s)$  denote nodal vectors originating from  $S$ ,  $B$  and  $E$ , respectively, and  $W$  is a dense and symmetric matrix corresponding to the operator  $\hat{W} \equiv \mu_0(\hat{Q} + 2\hat{I}/b)$ .

As the numerical method for solving the initial-value problem of (5), we adopt two types of ODE solvers: the backward Euler method and the Runge-Kutta method.

#### 3.1 Backward Euler method

After applying the backward Euler method to (5), we get the following discretized equations [1–3]:

$$\mathbf{G}_n(s^n) \equiv Ws^n + \Delta t e(s^n) - \mathbf{u}^n = \mathbf{0}, \quad (6)$$

where  $\Delta t$  is a time-step size and the superscript  $n$  indicates values at time  $t = n\Delta t$ . Furthermore,  $\mathbf{u}^n$  is a nodal vector irrelevant to  $s^n$ . Thus, the initial-boundary-value problem of (1) is transformed to the problem in which the nonlinear system  $\mathbf{G}_n(s) = \mathbf{0}$  is solved at the  $n$ th time step.

If the Newton method is applied to the nonlinear system  $\mathbf{G}_n(s) = \mathbf{0}$ , a linear system with a dense and symmetric matrix has to be solved at each iteration. Moreover, the matrix is indefinite and, hence, the Bunch-Kaufman factorization method [6] is adopted as a linear-system solver. Thus, the Newton method requires no more than  $O(N_n^3)$  operations at each iteration. Here,  $N_n$  is the number of nodes.

#### 3.2 Runge-Kutta method

When the 5th-order Runge-Kutta method [7] is applied to (5), only 6 evaluations of  $f(t, s)$  are needed at each time step. Thus,  $O(N_n^2)$  operations are executed at each time step of the Runge-Kutta method. In contrast,  $O(N_n^3)$  operations are necessary at each time step of the backward Euler method. Therefore, the Runge-Kutta method is expected to have a much higher speed than the backward Euler method. However, it is essentially an explicit scheme and, hence, it might cause the numerical instability. In order to suppress the instability, Fehlberg's adaptive step-size control algorithm [7] is incorporated to the Runge-Kutta method.

In order to quantitatively investigate the performance of the adaptive step-size control algorithm, let us define the execution rate: if the initial-value problem of (5) is successfully solved from  $t = 0$  to  $t = T/f$  without causing any overflow, the execution rate  $R_E$  is defined as  $R_E \equiv T/2$ . Especially when an overflow does not happen during two time period of  $I(t)$ ,  $R_E$  becomes equal to 100%. The execution rate is calculated for various values of the nonlinear strength  $N$  and is depicted in Fig. 1. The execution rate is equal to 100% for the case with  $N \leq 13$ , whereas the time evolution process is terminated due to an overflow for the case with  $N \geq 14$ . On the other hand, the nonlinear strength  $N$  has been usually chosen such that  $N \geq 16$  in the shielding current analysis of a HTS thin film [3]. In this sense, the adaptive step-size control algorithm is not applicable to the shielding current analysis.

For the purpose of improving the performance of the adaptive step-size control algorithm, we propose that the power law (2) be modified as follows:

$$E^*(j) = E_C(j/j_C)^{N^*(j/j_C)}. \quad (7)$$

Here,  $N^*(z)$  is given by

$$N^*(z) = (N - N_L)\varphi\left(\frac{4[z - (z_U + z_L)/2]}{(z_U - z_L)/2}\right) + N_L,$$

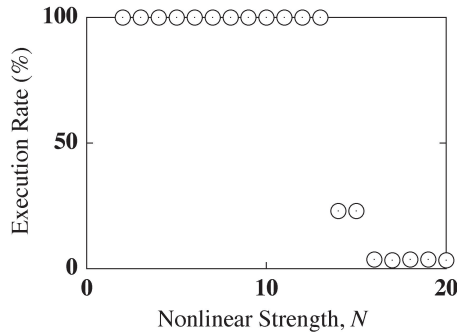


Fig. 1 Dependence of the execution rate  $R_E$  on the nonlinear strength  $N$  for the case with  $I_0 = 200$  mA and  $y_c = 0$  mm. Here, (2) is assumed as the  $J$ - $E$  constitutive relation.

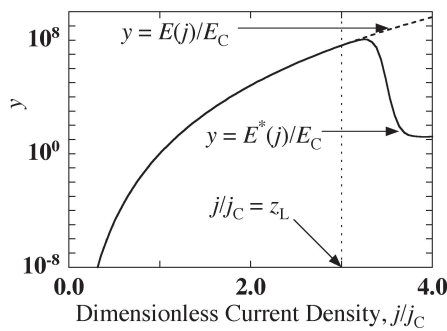


Fig. 2 The graphs of  $E^*(j)$  and  $E(j)$  for the case with  $z_L = 3$ ,  $z_U = 4$ ,  $N_L = 2$  and  $N = 16$ .

where  $z_L$ ,  $z_U$  and  $N_L$  are all constants and  $\varphi(x) \equiv (1 - \tanh x)/2$ . The graphs of  $E^*(j)$  and  $E(j)$  are shown in Fig. 2. We see from this figure that the equality  $E^*(j) = E(j)$  is approximately fulfilled for  $j/j_C \leq z_L$ . Hence, if the solution of (1) and (4) satisfies (3), it also becomes an approximate solution of (1) and (2). For this reason, we propose the following method for solving the initial-boundary-value problem of (1):

- 1) After assuming (4) and (7) as the  $J$ - $E$  constitutive relation, the initial-value problem of (5) is solved by means of the Runge-Kutta method with an adaptive step-size control algorithm;
- 2) Whether the resulting solution satisfies (3) or not is checked numerically. If the solution fulfills (3), it is acceptable as a solution of (1) and (2).

According to our experience of the shielding current analysis, the value of  $|j|/j_C$  never exceeds 3. Thus, the values of  $z_L$  and  $z_U$  are fixed as  $z_L = 3$  and  $z_U = 4$ . The execution rate  $R_E$  is evaluated as a function of  $N_L$  and is depicted in Fig. 3. Since the execution rate amounts to 100% for  $N_L \leq 11$ , we assume  $N_L = 2$  hereafter.

Let us compare the speed of the proposed method with that of the backward Euler method. The CPU times required for both methods are measured on NEC SX-8/8M1 of the LHD Numerical Analysis System in National Institute of Fusion Science. The dependence of the CPU time

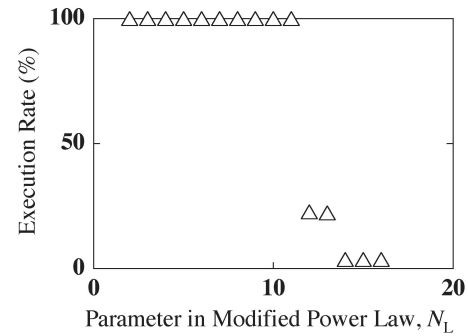


Fig. 3 Dependence of the execution rate  $R_E$  on the parameter  $N_L$  for the case with  $I_0 = 200$  mA,  $y_c = 0$  mm and  $N = 16$ .

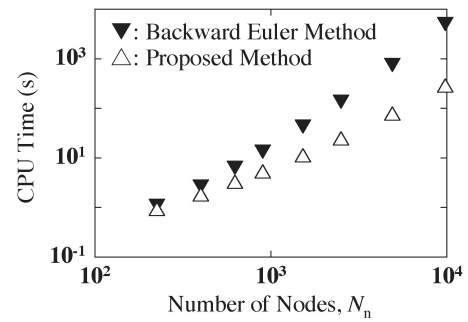


Fig. 4 Dependence of the CPU time on the number  $N_n$  of nodes for the case with  $I_0 = 50$  mA,  $y_c = 0$  mm and  $N = 16$ . Here, the initial-boundary-value problem of (1) is solved from  $t = 0$  to  $t = 37/(150f)$  by means of either the backward Euler method or the proposed method. In addition,  $\Delta t = 1/(150f)$  is used as a constant time-step size for the former, whereas it is chosen as an initial time-step size for the latter.

on the number of nodes is depicted in Fig. 4. This figure indicates that the proposed method is much faster than the backward Euler method. From this result, we can conclude that the proposed method becomes a powerful tool for solving the initial-boundary-value problem of (1).

By using the above method, we have developed a numerical code for analyzing the time evolution of the shielding current density.

## 4. Numerical Simulation

### 4.1 Inductive method and Mawatari's theory

The inductive method [4, 5] has been widely used as a contactless method for measuring  $j_C$  in a HTS thin film. In the method, an ac current  $I(t)$  is applied in a coil and, simultaneously, the third-harmonic voltage  $V_3 \sin(6\pi ft + \theta_3)$  induced in the coil is monitored. In general,  $V_3$  abruptly develops just after  $I_0$  exceeds the threshold current  $I_T$ .

Mawatari *et al.* theoretically analyzed the  $V_3$  generation to get the following formula [5]:

$$j_C^* = 2F(r_m)I_T/b, \quad (8)$$

where  $j_C^*$  is an estimated value of the critical current den-

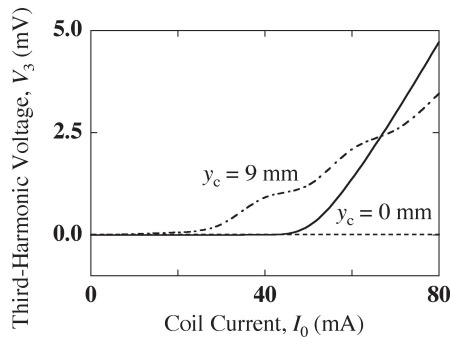


Fig. 5 The third-harmonic voltage  $V_3$  as functions of the coil current  $I_0$  for the case with  $N = 16$ .

sity. In addition,  $F_m$  is a factor determined only by the configuration of a coil and a film [5]. Equation (8) indicates that the critical current density can be estimated from the measured value of the threshold current  $I_T$ . However, in deriving (8), a HTS film is assumed to extend infinitely so that the film edge may not affect the spatial distribution of the shielding current density. In this sense, it is not unclear whether (8) is valid near the film edge.

## 4.2 Numerical simulation of inductive method

In this section, the edge effect of a HTS film on the inductive method is assessed by means of the numerical simulation. Since the coil-film configuration is given in section 2,  $F_m$  is easily evaluated as  $F_m = 6.23 \times 10^4 \text{ m}^{-1}$ .

Let us first investigate the influence of the coil position on the estimated value  $j_C^*$  of the critical current density. To this end,  $I_0$ - $V_3$  curves are determined for various values of  $y_c$  and the results of computations are depicted in Fig. 5. After applying the voltage criterion [5] ( $I_0 = I_T \iff V_3 = 0.1 \text{ mV}$ ) to the curves, we get  $I_T = 47.6 \text{ mA}$  and  $24.2 \text{ mA}$  for  $y_c = 0 \text{ mm}$  and  $9 \text{ mm}$ , respectively. By substituting the values of  $F_m$  and  $I_T$  into (8), we obtain  $j_C^* = 0.988 \text{ MA/cm}^2$  and  $0.503 \text{ MA/cm}^2$  for  $y_c = 0 \text{ mm}$  and  $9 \text{ mm}$ , respectively. Note that the assumed value of the critical current density is  $j_C = 1 \text{ MA/cm}^2$ . Hence, the accuracy of  $j_C^*$  becomes remarkably degraded as the coil position  $(x_c, y_c)$  approaches the film edge.

Next, we explain the cause of the accuracy degradation of  $j_C^*$  near the film edge. For this purpose, the spatial distributions of the shielding current density are numerically determined and are depicted in Figs. 6(a) and 6(b). The distribution is almost axisymmetric for  $y_c = 0 \text{ mm}$ , whereas it becomes anisotropic for  $y_c = 9 \text{ mm}$ . This result means that the axisymmetry of the shielding current density will be distorted with an approach of the coil to the film edge. On the other hand, Mawatari *et al.* assumed the axisymmetry of the shielding current density in deriving (8). Therefore, the accuracy degradation of  $j_C^*$  near the film edge is attributable to the lost of the axisymmetric distribution of the shielding current density.

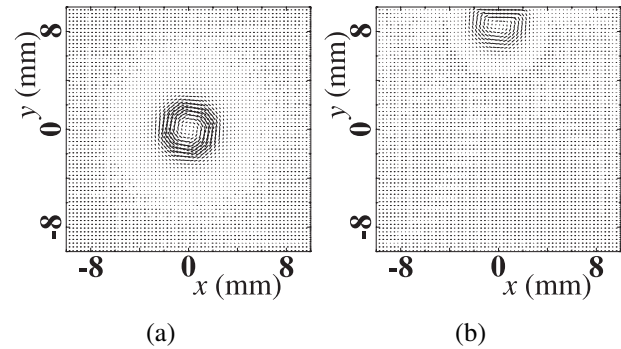


Fig. 6 Spatial distributions of the shielding current density at time  $t = 1.2/f$  for the case with  $I_0 = 50 \text{ mA}$  and  $N = 16$ . Here, (a)  $y_c = 0 \text{ mm}$  and (b)  $y_c = 9 \text{ mm}$ .

## 5. Conclusion

We have investigated the numerical method for calculating the shielding current density in a HTS thin film. After discretized with respect to space, the initial-boundary-value problem of the shielding current density is transformed to the first-order ODEs. However, owing to the strong nonlinearity, the ODEs cannot be always solved by the Runge-Kutta method with an adaptive step-size control. In order to resolve these difficulties, we have proposed the method in which the  $J$ - $E$  constitutive relation is slightly modified from the original one. A numerical code for analyzing the shielding current density has been developed on the basis of the proposed method and, as an application of the code, the inductive method has been investigated. Conclusions obtained in the present study are summarized as follows.

- 1) The proposed method has a much higher speed than the conventional backward Euler method. This tendency indicates that the proposed method can be a useful tool for the time-dependent analysis of the shielding current density in a HTS thin film.
- 2) The numerical simulation of the inductive method shows that, if the coil position is close to the film edge, the accuracy of the method becomes remarkably degraded. This is mainly because the distribution of the shielding current density becomes anisotropic around the symmetry axis of the coil.

- [1] A. Kamitani and S. Ohshima, IEICE Trans. Electron. **E82-C**, 766 (1999).
- [2] A. Kamitani, S. Ikuno and T. Yokono, IEICE Trans. Electron. **E87-C**, 101 (2004).
- [3] A. Kamitani, T. Takayama and S. Ikuno, IEEE. Trans. Magn. **44**, 926 (2008).
- [4] J. H. Claassen, M. E. Reeves and R. J. Soulen, Jr., Rev. Sci. Instrum. **62**, 996 (1991).
- [5] Y. Mawatari, H. Yamasaki and Y. Nakagawa, Appl. Phys. Lett. **81**, 2424 (2002).
- [6] J. R. Bunch, L. Kaufman and B. N. Parlett, Numer. Math. **27**, 95 (1976).
- [7] W. H. Press, S. A. Teukolsky, W. T. Vetterling and B. P. Flannery, *Numerical Recipes in Fortran 77, 2nd ed.* (Cambridge University Press, New York, 1992) Chap. 16.